International Journal of Nanomedicine

Dovepress
open access to scientific and medical research

Open Access Full Text Article

ORIGINAL RESEARCH

Bone Mesenchymal Stem Cells Origin Exosomes are Effective Against Sepsis-Induced Acute Kidney Injury in Rat Model

Cui Jin, Yongmei Cao, Yingchuan Li

Department of Critical Care Medicine, Shanghai Tenth People's Hospital, Tongji University School of Medicine, Shanghai, 200072, People's Republic of China

Correspondence: Yingchuan Li, Department of Critical Care Medicine, Shanghai Tenth People's Hospital, Tongji University School of Medicine, Shanghai, 200072, People's Republic of China, Email yingchuan_li@tongji.edu.cn

Introduction: The incidence and mortality rates of sepsis-induced acute kidney injury (SAKI) remain high, posing a substantial healthcare burden. Studies have implicated a connection between the development of SAKI and inflammation response, apoptosis, and autophagy. Moreover, evidence suggests that manipulating autophagy could potentially influence the prognosis of this condition. Notably, exosomes derived from bone mesenchymal stem cells (BMSCs-Exo) have exhibited promise in mitigating cellular damage by modulating pathways associated with inflammation, apoptosis, and autophagy. Thus, this study aims to investigate the influence of BMSCs-Exo on SAKI and the potential mechanisms that drive this impact.

Methods: The SAKI model was induced in HK-2 cells using lipopolysaccharide (LPS), while rats underwent cecal ligation and puncture (CLP) to simulate the condition. Cell viability was assessed using the CCK-8 kit, and kidney damage was evaluated through HE staining, blood urea nitrogen (BUN), and serum creatinine (SCr) measurements. Inflammatory-related RNAs and proteins were quantified via qPCR and ELISA, respectively. Apoptosis was determined through apoptosis-related protein levels, flow cytometry, and TUNEL staining. Western blot analysis was utilized to measure associated protein expressions.

Results: In vivo, BMSCs-Exo ameliorated kidney injury in CLP-induced SAKI rats, reducing inflammatory cytokine production and apoptosis levels. Fluorescence microscope observed the absorption of BMSCs-Exo by renal cells following injection via tail vein. In the SAKI rat kidney tissue, there was an upregulation of LC3-II/LC3-I, p62, and phosphorylated AMP-activated protein kinase (p-AMPK) expressions, indicating blocked autophagic flux, while phosphorylated mammalian target of rapamycin (p-mTOR) expression was downregulated. However, BMSCs-Exo enhanced LC3-II/LC3-I and p-AMPK expression, concurrently reducing p62 and p-mTOR levels. In vitro, BMSCs-Exo enhanced cell viability in LPS-treated HK-2 cells, and exerted anti-inflammation and anti-apoptosis effects which were consistent with the results in vivo. Similarly, rapamycin (Rapa) exhibited a protective effect comparable to BMSCs-Exo, albeit partially abrogated by 3-methyladenine (3-MA).

Conclusion: BMSCs-Exo mitigate inflammation and apoptosis through autophagy in SAKI, offering a promising avenue for SAKI treatment.

Keywords: exosomes, bone mesenchymal stem cells, acute kidney injury, sepsis, autophagy

Introduction

Acute kidney injury (AKI) is a multifaceted condition characterized by a rapid decline in kidney function. Epidemiological analysis underscores various factors that can trigger AKI, encompassing sepsis, toxins, ischemia, and trauma.[1] Notably, sepsis accounts for nearly half of all AKI instances, with sepsis-induced acute kidney injury (SAKI) bearing a daunting 70% mortality rate.[2,3] Pathogen invasion triggers the recognition of pathogen-associated molecular patterns (PAMPs), subsequently instigating the release of damage-associated molecular patterns (DAMPs). These molecular events drive inflammatory cascades in the sepsis process, culminating in excessive inflammation-induced

Received: 14 August 2023
Accepted: 13 December 2023
Published: 18 December 2023

Graphical Abstract

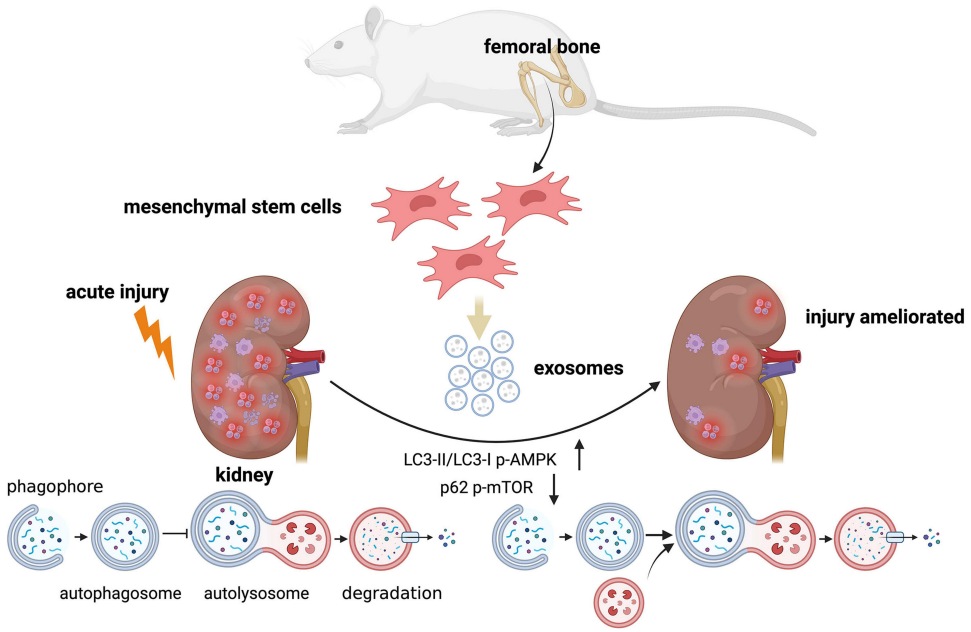

cell apoptosis and the exacerbation of renal injury.[4–6] A wealth of evidence supports the mitigation of SAKI through the suppression of inflammation and apoptosis.[7,8]

Exosomes, nano-sized endosome-derived extracellular vesicles, are rich in proteins, lipids, mRNAs, and microRNAs (miRNAs).[9] These vesicles have been implicated in signal transmission,[10] antigen presentation,[11] and immune response modulation.[12] Moreover, mounting evidence underscores the role of exosomes in kidney disorders, including IgA nephropathy,[13,14] nephrotic syndrome,[15] AKI, and chronic kidney disease (CKD).[16–18] BMSCs-Exo manifest a spectrum of effects, encompassing tissue repair regulation[19] and regeneration.[20] Zhu et al demonstrated that BMSCs-Exo mitigate kidney ischemia/reperfusion (I/R) injury by conveying miR-199a-3p to tubular cells, thereby inhibiting apoptosis.[21] However, it remains uncertain whether BMSCs-Exo can impact SAKI and its underlying mechanisms.

Autophagy, a prototypical cellular pathway, orchestrates the recycling of damaged organelles and cellular components to maintain cell and tissue homeostasis. Extensive research has illuminated autophagy's multifaceted regulation, involving an intricate interplay between inflammation and apoptosis.[22–24] In macrophages, autophagy induction has been proposed to exert an anti-inflammatory effect, while inhibition of autophagy has been linked to enhanced apoptosis.[25,26] Many studies have indicated that autophagy takes part in the recovery of kidney during AKI.[27] For example, a recent study has revealed that berberine could mitigate contrast-induced acute kidney injury through regulating autophagy.[28] Target of rapamycin (TOR), a serine/threonine protein kinase, negatively regulates autophagy levels. Nutrient scarcity or stress triggers autophagy initiation through dephosphorylation of the mammalian target of rapamycin (mTOR) site.[22,29] Additionally, AMP-activated protein kinase (AMPK) modulates this process through diverse mechanisms, including TSC2 phosphorylation to suppress mTOR activity.[30,31] Notably, exosomes have emerged as regulators of autophagy, influencing disease outcomes.[32] Ji et al have reported that exosomes isolated from synovial fluid could relieve osteoarthritis by delivering miR-182-5p to promote autophagy.[33]

In this study, the SAKI model was established using lipopolysaccharide (LPS)-treated HK-2 cells and Cecal Ligation and Puncture (CLP) in rats. Subsequently, we investigated the impact of BMSCs-Exo on cell apoptosis, inflammation,

and autophagy levels. The primary objective of this research was to ascertain whether BMSCs-Exo confer renoprotective effects on SAKI and to elucidate the associated mechanisms.

Materials and Methods

Cell Culture Studies

Bone mesenchymal stem cells (BMSCs) and the human renal tubular epithelial cell line HK-2 were procured from the Stem Cell Bank of the Chinese Academy of Sciences. The HK-2 cells underwent STR authentication through Shanghai Biowing Applied Biotechnology Co. LTD, located in Shanghai, China. BMSCs and HK-2 cells were cultured in α-MEM (Gibco) and Dulbecco's modified Eagle's medium/nutrient mixture F-12 (DMEM/F12, Gibco), respectively, supplemented with 10% fetal bovine serum (FBS, Gibco) and 100 U/mL streptomycin-penicillin (Gibco). The incubation was performed at 37°C in a humidified atmosphere with 5% CO2 and 95% air. BMSCs at passages 3 to 5 were selected for subsequent experimentation. Upon reaching optimal density, HK-2 cells were subjected to varying concentrations of LPS (Sigma-Aldrich) (0–500 μg/mL) for different durations (0–72 h). In the case of rapamycin and chloroquine treatments, HK-2 cells were exposed to 5 μmol/L rapamycin for 24 h and 20 μmol/L chloroquine for 24 h, respectively.

Isolation and Characterization of Exosomes

Upon reaching 90% confluence, the conditioned medium of BMSCs was harvested and subjected to sequential centrifugation steps at 300 ×g (10 min), 3000 ×g (10 min), and 10,000 ×g (30 min) at 4 °C. Following removal of the resultant pellet, the supernatant was passed through a 0.22 μm filter (Millipore) and subsequently subjected to ultracentrifugation at 110,000 ×g for 70 min at 4 °C. The ensuing white precipitates at the base of the centrifuge tube constituted the exosomal fraction. The ultimate pellet was reconstituted in PBS and preserved at −80 °C for subsequent applications. Protein quantification of the concentrated exosomes was carried out using the BCA protein assay kit (Beyotime). Morphological examination of the exosomes was conducted via transmission electron microscopy (FEI). The dimensions and relative abundance of exosomes were evaluated utilizing nanoparticle tracking analysis (NTA) via ZetaView PMX110 (Particle Metrix). Immunoblotting was employed for the detection of CD9, CD63, CD81, and Calnexin proteins.

Cell Viability Assay

Cell viability was assessed using the CCK-8 reagent (Dojindo), following the guidelines provided by the manufacturer. In brief, cells were plated in 96-well plates and subsequently treated. Post-treatment, each well received 10 μL of CCK-8 solution, followed by an incubation period of 1 to 4 hours. The resulting optical density (OD) was measured at 450 nm utilizing a microplate reader.

Enzyme Linked Immunosorbent Assay (ELISA)

Cell culture supernatants were harvested and subsequently stored at −20°C for the subsequent cytokine analysis. Levels of proinflammatory cytokines (TNF-α, IL-6, IL-1β) in the supernatant were quantified using an enzyme-linked immunosorbent assay (ELISA) kit, following established protocols. Absorbance readings at 450 nm were obtained using a microplate reader.

Flow Cytometry

The apoptosis rate of HK-2 cells was assessed using the Annexin V-FITC Apoptosis Detection Kit (Beyotime). HK-2 cells from different experimental groups were harvested and suspended in 195 μL of Annexin V-FITC binding buffer. Subsequently, 5 μL of Annexin V-FITC and 10 μL of propidium iodide (PI) were introduced to the cell suspension. Following a 20-minute incubation in a dim environment, cell samples were promptly subjected to flow cytometry (Beckman). The apoptotic cell percentage was calculated by summing the percentages of cells in the Q2-2 and Q2-4 quadrants.

Animal

All the procedures were confirmed to the Institutional Animal Care and Use Committee of the Shanghai Jiao Tong University Affiliated Sixth People's Hospital [No: DWLL2023-0421] and were conducted according to the Research Guide for the Care and Use of Laboratory Animals. Adult male Sprague-Dawley rats (200–250 g, SPF) were subjected to random allocation into three distinct experimental groups, each tailored to specific study requirements: (1) the sham group (n=4), which underwent all procedures except cecal ligation and puncture (CLP); (2) the CLP group (n=4), subjected to CLP induction; and (3) the CLP+Exo group (n=4), wherein exosomes (100 μg, 3 h post CLP) were administered via the tail vein subsequent to CLP. The remaining cohort of 30 animals was reserved for subsequent survival analysis.

CLP-Induced SAKI

Rats were anesthetized with pentobarbital sodium (50 mg/kg) through intraperitoneal injection. Following aseptic preparation, a midline laparotomy incision of 2 cm was created on the abdominal region. Subsequently, a 50% cecal ligation was performed, and the cecum was gently exteriorized, followed by a 1 mm puncture using a needle to initiate sepsis induction. A small amount of cecal contents was extruded before carefully returning the cecum into the peritoneal cavity. The abdominal incision was meticulously sutured. Post-procedure, rats were resuscitated with 20 mL/kg of saline solution. The successful establishment of the model was judged by whether BUN, SCr and inflammatory factors were significantly increased, and whether kidney damage could be observed pathologically.

Tracking of Administered Exosomes

For in vitro monitoring of BMSCs-Exo uptake by HK-2 cells, DiI-labeled exosomes at a concentration of 10 μmol/L were introduced to HK-2 cells and incubated for 4 hours. Subsequently, the cells were rinsed with phosphate-buffered saline (PBS, Servicebio) and then fixed using 4% paraformaldehyde (PFA, Servicebio). F-actin was visualized by staining with FITC-phalloidin (Servicebio), while DAPI (Servicebio) was employed to stain the cell nuclei. To trace BMSCs-Exo uptake by the kidney in vivo, 10 μmol/L DiI-labeled exosomes were administered post-CLP induction, and kidney sections were subjected to DAPI staining to visualize the absorbed exosomes. Imaging of the stained samples was performed using a fluorescence microscope (Leica).

HE Staining

Kidneys were fixed in paraformaldehyde (PFA) and embedded in paraffin for subsequent processing. Hematoxylin and eosin staining was performed to visualize the tissue. The tubular injury score was determined by evaluating the extent of tubular vacuolization, employing blind analysis at a magnification of 200×.

Quantitative Reverse Transcription Polymerase Chain Reaction (qRT-PCR)

Total mRNA was extracted from both HK-2 cells and rat kidneys using the EZ-press RNA Purification Kit (EZBioscience). Reverse transcription of mRNA into cDNA was accomplished using the Color Reverse Transcription Kit (EZBioscience). Subsequently, quantitative real-time polymerase chain reaction (qRT-PCR) was performed using the 2× Color SYBR Green qPCR Master Mix (EZBioscience) and analyzed using the LightCycler 480 II system (Roche). The relative quantification of mRNA was normalized to glyceraldehyde 3-phosphate dehydrogenase (GAPDH) following the $2^{-\Delta\Delta Ct}$ method. The primer sequences for the mRNAs are detailed in Table 1.

Western Blot

Protein extraction was performed using radioimmunoprecipitation assay (RIPA) buffer (Solarbio). Subsequently, the total protein concentration was determined using BCA protein assay kits (Beyotime). A volume equivalent to 1/4 of the supernatant was mixed with 5× sodium dodecyl sulfate (SDS) loading buffer (Epizyme) and heated in boiling water at 100°C for 10 minutes. The resulting protein samples were loaded in equal amounts, separated through sodium dodecyl sulfate-polyacrylamide gel electrophoresis (SDS-PAGE), and subsequently transferred onto polyvinylidene difluoride

Table 1 The Primer Sequences of mRNAs TNF-α, IL-6 and IL-1β

Gene Name	Primers
Human-TNF-α	(F) 5'-TGGCGTGGAGCTGAGAGATAACC-3'
	(R) 5'-CGATGCGGCTGATGGTGCGG-3'
Human-IL-6	(F) 5'-CACTGGTCTTTTGGAGTCTGAG-3'
	(R) 5'-GGACTTTTGTACTCATCCGCAC-3'
Human-IL-1β	(F) 5'-GCCAGTGAAATGATGGCCTATC-3'
	(R) 5'-AGGAGCACTTCATCTGTCTAGG-3'
Human-GAPDH	(F) 5'-ACAACTTTGGTATsCGTGGAAGG-3'
	(R) 5'-GCCATCACGCCACAGTTTC-3'
Rat-TNF-α	(F) 5'-TGATCCGAGATGTGGAACTG-3'
	(R) 5'-CGAGCAGGAATGAGAAGAGG-3'
Rat-IL-6	(F) 5'-AATCTCACAGCAGCATCTCGACAAG-3'
	(R) 5'-TCCACGGGCAAGACATAGGTAGC-3'
Rat-IL-1β	(F) 5'-TGACCCATGTGAGCTGAAAG-3'
	(R) 5'-AGTTGGGGAACTGTGCAGAC-3'
Rat-GAPDH	(F) 5'-GACATGCCGCCTGGAGAAAC-3'
	(R) 5'-AGCCCAGGATGCCCTTTAGT-3'

(PVDF) membranes. Following a 10-minute blocking step with protein-free rapid blocking buffer (Epizyme) at room temperature (RT), the membranes were subjected to overnight incubation with primary antibodies, including anti-CD9 (bs-2489R, Bioss), anti-CD63 (AF5117, Affinity), CD81 (DF2306, Affinity), anti-Calnexin (AF5362, Affinity), anti-Cleaved-caspase 3 (9664T, CST), anti-Bax (2772T, CST), anti-Bcl2 (4223T, CST), anti-LC3 (AF5402, Affinity), anti-p62 (AF5384, Affinity), anti-p-AMPK (2535S, CST), anti-AMPK (5831S, CST), anti-p-mTOR (AF3308, Affinity), anti-mTOR (AF6308, Affinity), and anti-β-actin (AC002, CST), all incubated at 4°C. Subsequently, HRP-conjugated anti-mouse (GB23301, Servicebio) and anti-rabbit (7074S, CST) secondary antibodies were applied for 2 hours at RT. Finally, membrane detection was conducted using the enhanced chemiluminescence (ECL) kit (Epizyme).

TUNEL Staining

Kidney tissues were meticulously fixed, dehydrated, and embedded onto prepared slides, which were subsequently subjected to de-paraffinization and rehydration. Following these steps, TUNEL staining was executed using a TUNEL kit (Servicebio), adhering to the manufacturer's guidelines. The nuclei were then counterstained with DAPI (Servicebio).

Statistical Analysis

All measurement data were presented as mean ± standard deviation (SD). Variations among group pairs were assessed using either Student's *t*-test or one-way analysis of variance (ANOVA). Statistical analysis was performed utilizing SPSS 24.0 software and GraphPad Prism 8. A p-value of less than 0.05 was regarded as indicative of statistical significance.

Results

BMSCs-Exo Could Be Absorbed by the Kidney to Exert a Protective Effect in SAKI Rats

In our prior investigations, BMSCs-Exo (with diameters ranging from 30 to 200 nm) were successfully isolated through ultracentrifugation. Subsequent investigations revealed the potential of BMSCs-Exo to mitigate inflammation and apoptosis induced by LPS in HK-2 cells (Supporting Materials 1 and 2De).[34] To explore the potential protective effects of BMSCs-Exo against SAKI in vivo, we established a SAKI rat model through CLP, followed by administration of BMSCs-Exo. Histopathological assessment using HE staining revealed a notably higher pathological score in the kidney tubules of the CLP group compared to the Sham group, with this effect being attenuated by BMSCs-Exo treatment (Figure 1A and B). Similarly, BMSCs-Exo treatment resulted in a reduction of BUN (mg/dL) and SCr (μmol/L) levels in SAKI rats induced by CLP (Figure 1C and D). Survival analysis (Figure 1E) depicted a progressive decline in the

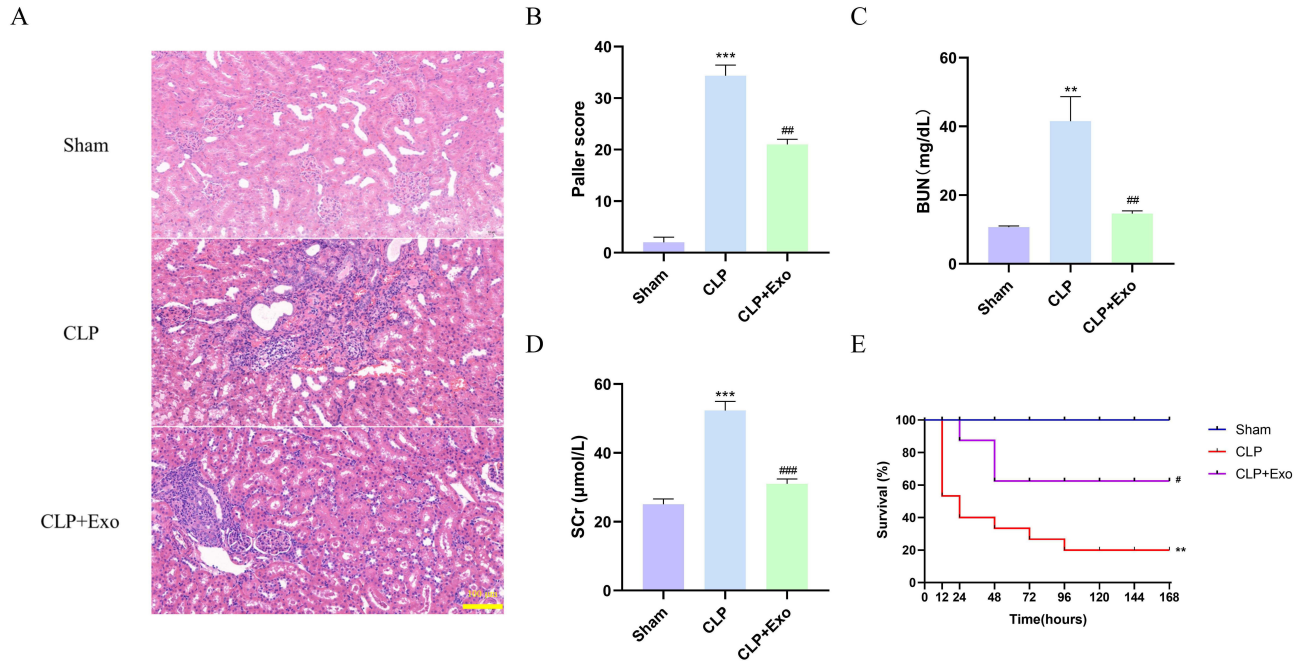

Figure 1 BMSCs-Exo alleviated sepsis-induced acute kidney injury. (**A** and **B**) HE staining was used to detect kidney tissue morphology. (**C** and **D**) BUN and SCr in the serum of rats were measured. (**E**) Survival rates were recorded. $^{**}P< 0.01$ and $^{***}P< 0.001$ vs Sham. $^{\#}P< 0.05$, $^{\#\#}P< 0.01$ and $^{\#\#\#}P<0.001$ vs CLP.

number of surviving rats over the 96-hour period in the CLP group, in contrast to the Sham group where all rats survived. Notably, BMSCs-Exo administration substantially enhanced the survival rate, yielding a significant difference between the CLP group and the CLP+Exo group (assessed via the Log rank test, $P < 0.05$). To ascertain the functional interaction of BMSCs-Exo within rat renal cells, a two-step approach was employed. Initially, BMSCs-Exo were pre-labeled with DiI before injection. Subsequently, SAKI rats were administered DiI-labeled exosomes. Finally, rat kidneys were harvested, followed by staining with phalloidin and DAPI. The visualization in Figure 2 distinctly illustrates the presence of a fluorescence signal emanating from DiI-labeled BMSCs-Exo within the kidney.

BMSCs-Exo Relieved the Inflammation and Apoptosis Level of SAKI Rats

Having demonstrated BMSCs-Exo's ability to mitigate LPS-induced inflammation and apoptosis in HK-2 cells, we proceeded to investigate whether BMSCs-Exo could exert a comparable effect in the SAKI rat model. The mRNA expression of

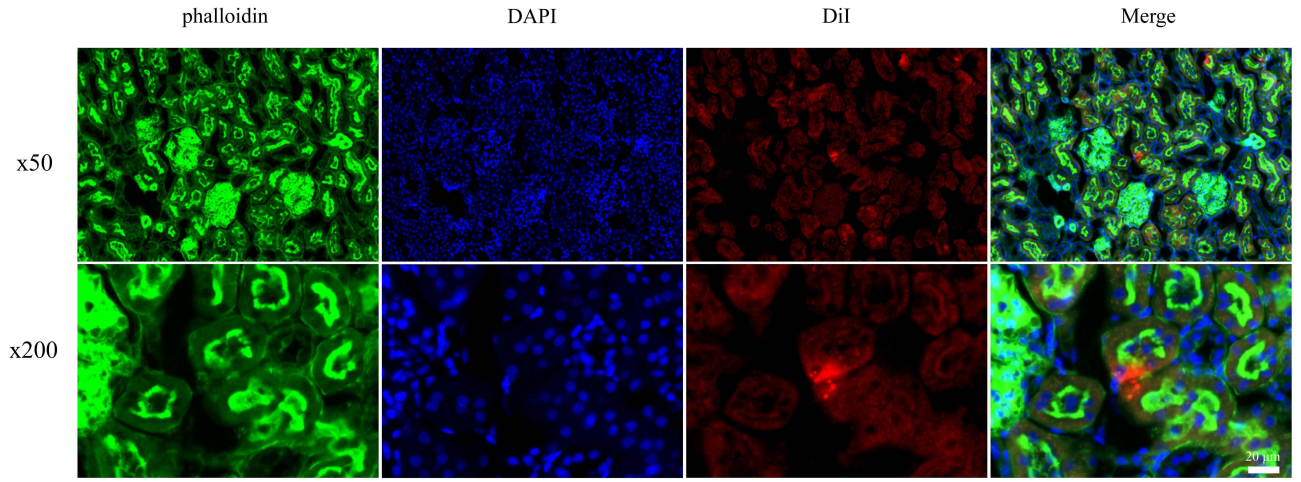

Figure 2 The uptake of BMSCs-Exo by renal cells. BMSCs-Exo were labeled with DiI (red). Renal cells were stained with phalloidin (green), and nuclei were counterstained with DAPI (blue).

pro-inflammatory cytokines TNF-α, IL-6, and IL-1β exhibited a significant increase in the CLP group, a response that was effectively countered by BMSCs-Exo treatment (Figure 3A–C). Notably, in SAKI rats, there was an elevation in Cleaved caspase-3 and Bax expression, accompanied by down-regulation of the anti-apoptotic protein bcl2. In contrast, BMSCs-Exo intervention led to a decline in Cleaved caspase-3 and Bax expression, and an increase in bcl2 expression (Figure 3D–G). Similarly, apoptotic levels showed an upward trend in the CLP group, which was subsequently mitigated in the CLP+Exo group (Figure 3H).

BMSCs-Exo Promoted Autophagic Flux via the AMPK/mTOR Pathway in SAKI Rats

This study delved into the intricate interplay between autophagy and the impact of BMSCs-Exo on SAKI in vivo. A marked elevation in the expression of LC3-II/LC3-I and p62 was observed within the CLP group when contrasted with the Sham group. Notably, in the CLP+Exo group, the expression of LC3-II/LC3-I increased, while that of p62 decreased,

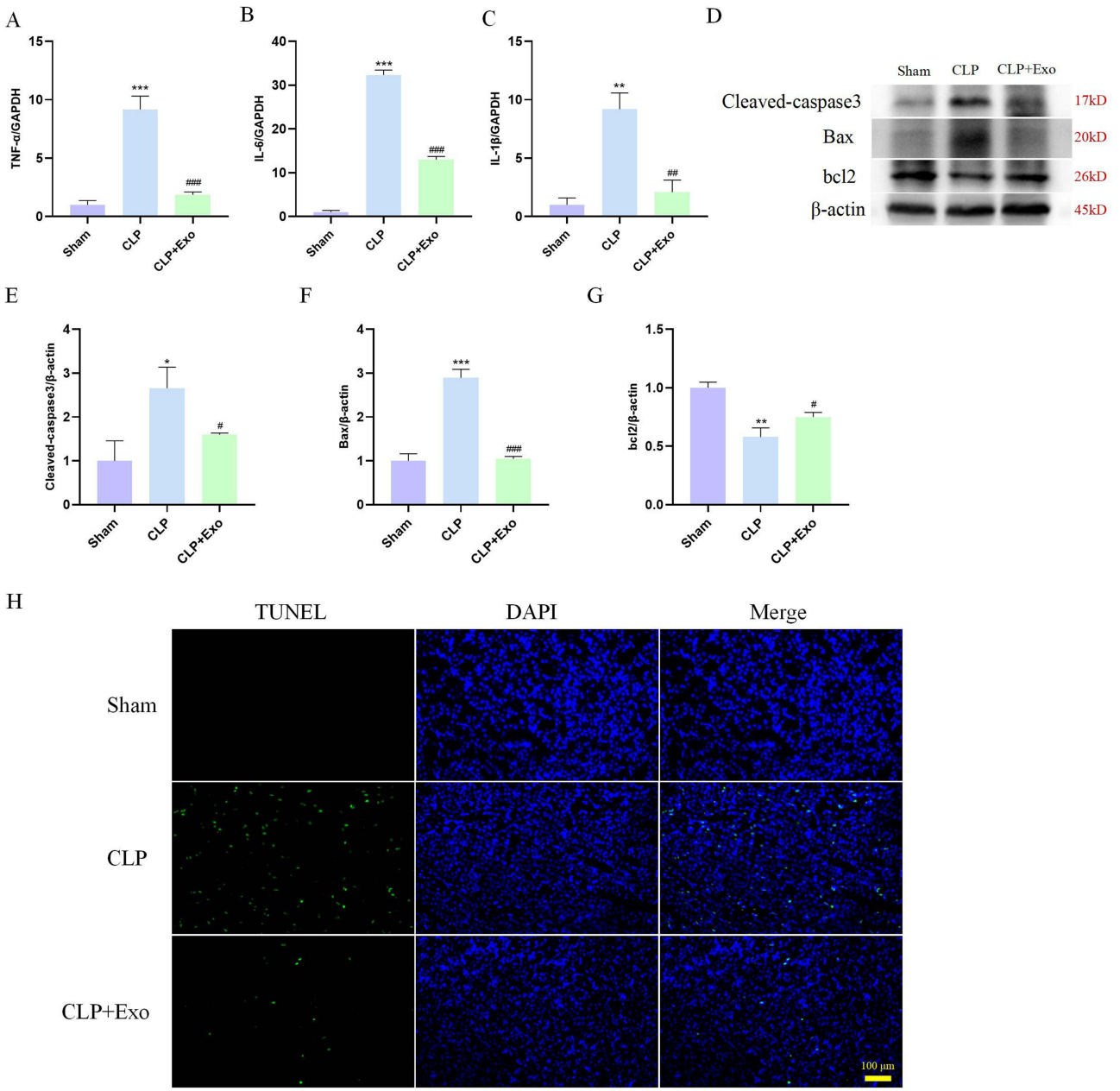

Figure 3 Effects of BMSCs-Exo on inflammation and apoptosis of rat kidney. (**A**–**C**) The expression of TNF-α, IL-6, and IL-1β mRNA in kidney tissue was detected by ELISA. (**D**–**G**) The expression of Cleaved-caspase 3, Bax, and bcl2 protein was assessed by Western blot. (**H**) The apoptosis of kidney tissue was detected by TUNEL staining. **P*< 0.05, ***P*< 0.01 and ****P*< 0.001 vs Sham. $^{\#}$*P*< 0.05, $^{\#\#}$*P*< 0.01 and $^{\#\#\#}$*P*<0.001 vs CLP.

signifying a regulatory effect of BMSCs-Exo on autophagy (Figure 4A–C). Further elucidation of the underlying autophagic modulation mechanism by BMSCs-Exo involved a thorough examination of key autophagy regulators, namely AMPK and mTOR, within the kidney tissues of the Sham, CLP, and CLP+Exo groups. The findings demonstrated that p-AMPK and p-mTOR expressions were respectively up-regulated and down-regulated in kidney tissues of septic rats, in comparison to the Sham group. Remarkably, BMSCs-Exo intervention was associated with an augmented expression of p-AMPK and a diminished expression of p-mTOR, solidifying its role in activating the AMPK/mTOR-mediated autophagic flux pathway in the context of SAKI (Figure 4A, D–G).

LPS Decreased the Viability of HK-2 Cells

To unravel the underlying mechanism in vitro, varied concentrations of LPS (1, 10, 100, or 500 μg/mL) were employed to treat HK-2 cells over durations of 24, 48, and 72 hours. The results unequivocally exhibited a discernible temporal and dose-dependent decline in the viability of HK-2 cells subsequent to LPS exposure (Figure 5 A–E). Specifically, in comparison to the control group, the viability of HK-2 cells reduced to 88.4%, 66.8%, and 57.3% at 24, 48, and 72 hours, respectively, under LPS treatment (100 μg/mL). Furthermore, corresponding viability rates for HK-2 cells plunged to 71.7%, 35.2%, and 16.4% when the LPS dose escalated to 500 μg/mL. Remarkably, a substantial decrement in cell viability was observed at 100 μg/mL LPS concentration for 24 hours, thereby prompting the selection of LPS at 100 μg/mL for 24 hours as the optimal condition for subsequent experiments.

BMSCs-Exo Attenuated Inflammatory Response by Modulating Autophagy in HK-2 Cells

To further ascertain whether the anti-inflammatory action of BMSCs-Exo is mediated through autophagy modulation, we employed rapamycin (Rapa) and chloroquine (CQ) as autophagy activator and inhibitor, respectively. The outcomes of qRT-PCR analysis demonstrated that Rapa (an mTOR inhibitor promoting autophagy) elicited effects akin to those of

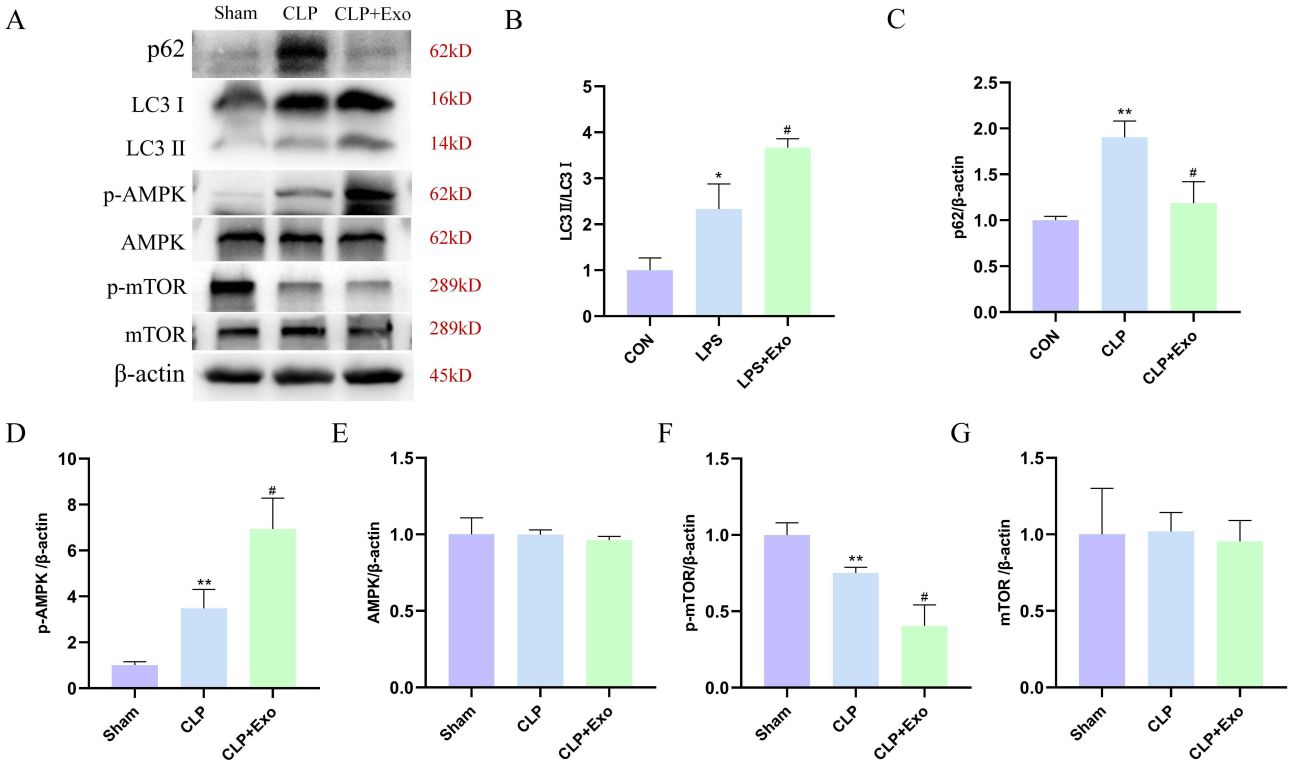

Figure 4 BMSCs-Exo modulated autophagy by regulating the AMPK/mTOR pathway. (**A**) Western blot was used to detect the expression of LC3-II/LC3-I, p62, p-AMPK, AMPK, p-mTOR, and mTOR protein in the kidney tissues. (**B–G**) Statistical results of expression in (**A**). *P< 0.05, **P< 0.01 vs Sham. #P< 0.05, vs CLP.

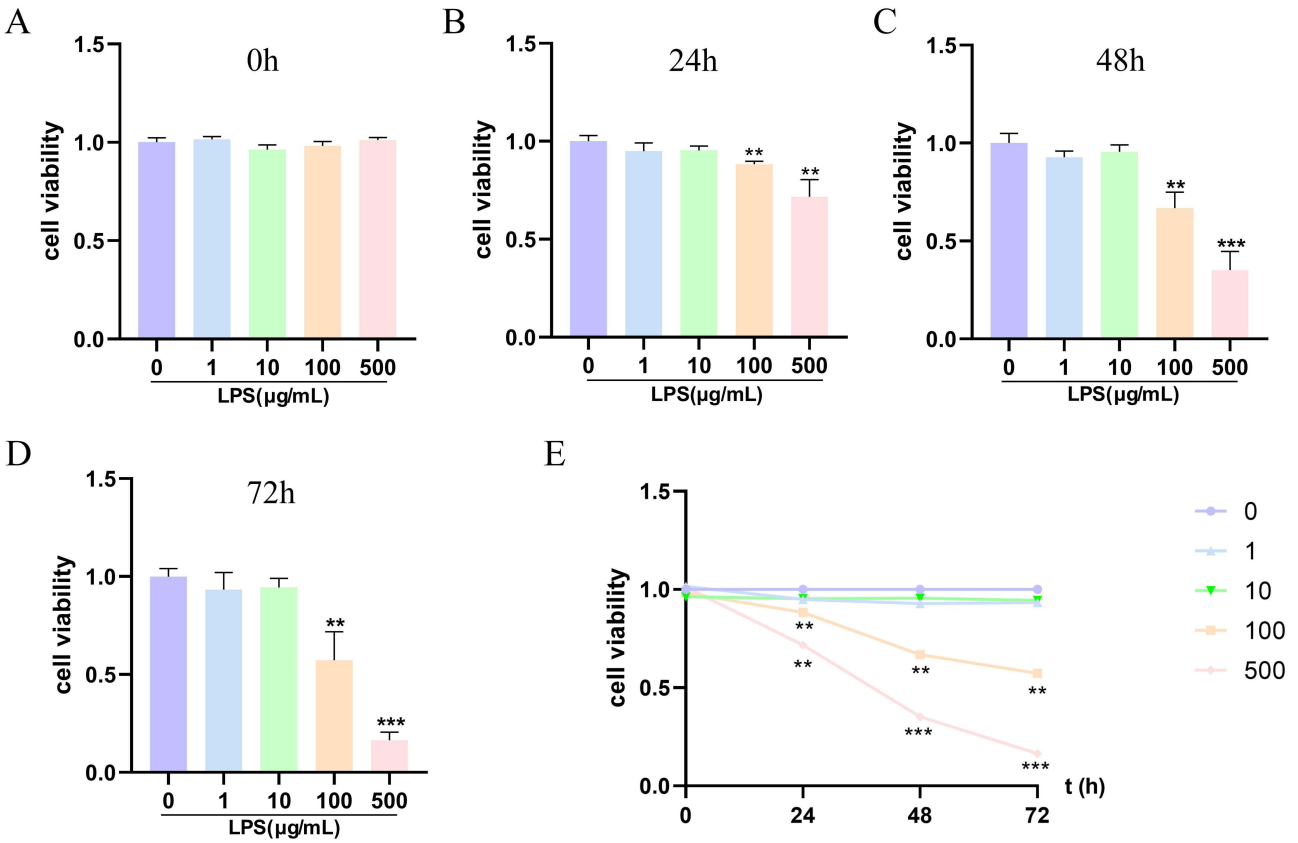

Figure 5 Effects of LPS on the cell viability of HK-2 cells. (**A**–**E**) HK-2 cell viability was detected by CCK-8 assay at different concentrations of LPS for 0, 24, 48, and 72 h. ***P*<0.01, and ****P*<0.001 vs 0 h.

BMSCs-Exo, mirrored in the alteration of TNF-α, IL-6, and IL-1β expressions. In contrast, the impact of BMSCs-Exo on TNF-α, IL-6, and IL-1β expressions was counteracted by CQ (Figure 6A–C). Furthermore, ELISA corroborated these qRT-PCR findings (Figure 6D–F). Collectively, these findings strongly suggest that BMSCs-Exo mitigates inflammatory responses through autophagy promotion, and this effect can be disrupted by inhibition of autophagy.

BMSCs-Exo Attenuated Apoptosis by Modulating Autophagy in HK-2 Cells

Likewise, to further elucidate whether BMSCs-Exo influences apoptosis via autophagy modulation, we employed Rapa and CQ to respectively trigger and suppress autophagy. In contrast to the LPS+Exo group, the addition of CQ in the LPS +Exo+CQ group substantially augmented the levels of Cleaved-caspase 3 and Bax proteins (pro-apoptotic factors), while concurrently attenuating the expression of the anti-apoptotic factor, bcl2. This discernible effect of CQ counteracted the protective influence of BMSCs-Exo. Furthermore, Rapa exhibited commensurate effects with those of BMSCs-Exo (Figure 7A–D), whereas CQ impaired the impacts of BMSCs-Exo on apoptosis and cellular viability (Figure 7E–G). Collectively, these findings underline that BMSCs-Exo counteract cell apoptosis through autophagy promotion, a process which is susceptible to disruption by the autophagy inhibitor.

Discussion

In this study, we systematically investigated the impact of BMSCs-Exo on both in vivo and in vitro models of SAKI. Moreover, we delved into the underlying mechanisms, specifically focusing on the potential modulation of autophagy through the AMPK and mTOR pathways. Our findings unveiled a multifaceted protective role of BMSCs-Exo: they attenuated inflammatory responses in LPS-treated HK-2 cells, marked by the downregulation of TNF-α, IL-6, and IL-1β, alongside reduced apoptosis. Further, our investigations extended to an in vivo context, where BMSCs-Exo demonstrated renoprotective effects in a rat model of SAKI. Firstly, we established that BMSCs-Exo ameliorated kidney pathology and

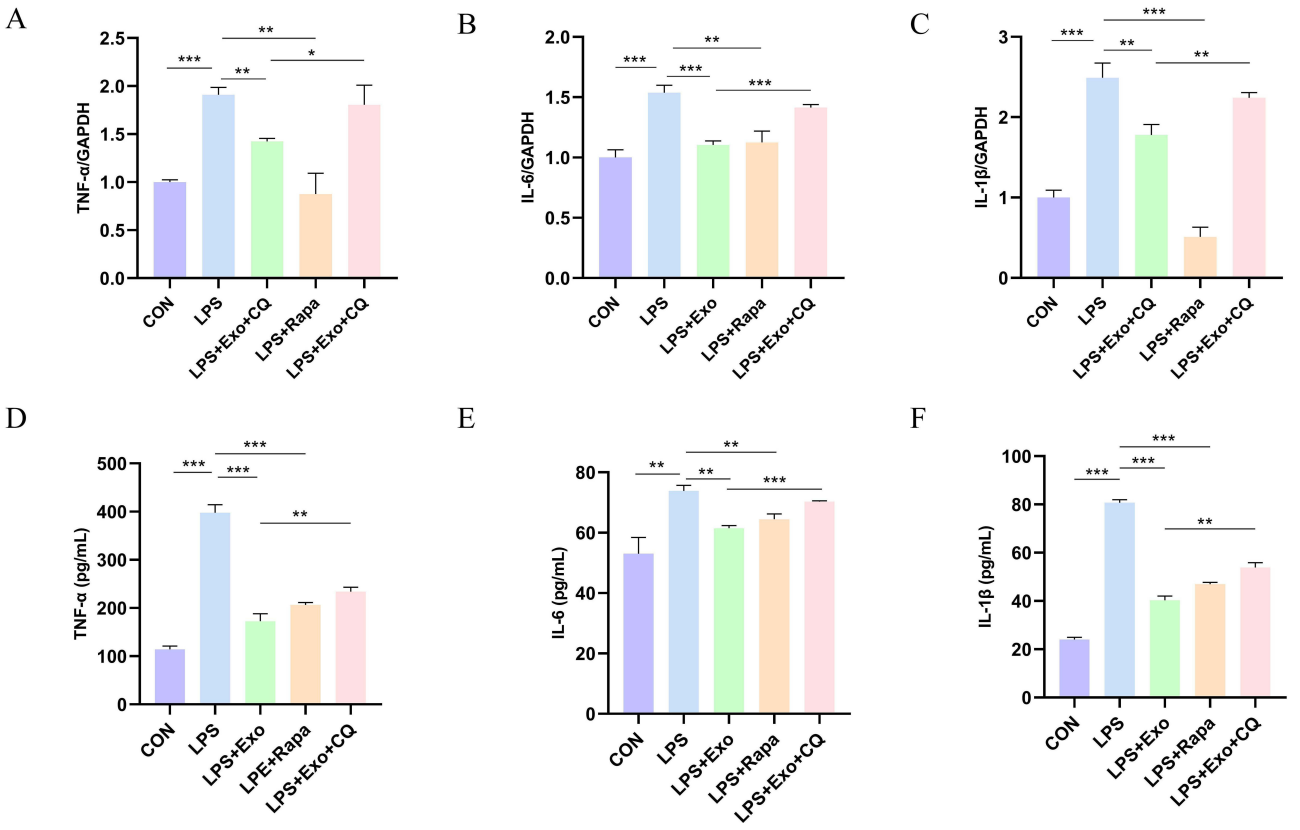

Figure 6 Evaluation of the role of Rapa and CQ on the anti-inflammatory effect of BMSCs-Exo. (**A**–**C**) qRT-PCR was applied to test mRNAs of TNF-α, IL-6, and IL-1β in five groups. GAPDH was used as an internal control. (**D**–**F**) The concentration of TNF-α, IL-6, and IL-1β in the cell supernatants of each group was detected using the corresponding ELISA kit. *P< 0.05, **P< 0.01 and ***P< 0.001.

restored renal function in septic rats. Subsequently, we substantiated their anti-inflammatory and anti-apoptotic prowess in the SAKI rat model. Lastly, we corroborated these effects by linking them to the augmentation of autophagic flux and the activation of the AMPK/mTOR pathway.

Mesenchymal stem cells, initially identified within the bone marrow, possess the remarkable capacity for self-renewal and differentiation under specific conditions.[35] Among various cell types, including mesenchymal stem cells, the secretion of exosomes is a notable phenomenon, enabling the transfer of bioactive molecules like proteins, lipids, mRNAs, and microRNAs (miRNAs) to target cells.[36,37] The contents of exosomes depend on the cell origin, condition, et. Sepsis is essentially an inflammatory cascade caused by the imbalance between pro-inflammatory and anti-inflammatory response. When pro-inflammation is in a dominant position, a large number of inflammatory factors are released to attack various organs of the body, notably the kidneys. The diagnostic and therapeutic roles of exosomes in sepsis and sepsis-induced organ injury have been reported.[38,39] Noteworthy studies have shed light on the protective attributes of exosomes derived from adipose tissue mesenchymal stem cells (AMSCs-Exo) against SAKI by activating the SIRT1 pathway in murine models[40] (Gao et al). Similarly, exosomes originating from human umbilical cord mesenchymal stem cells (HucMSCs-Exo) have been found to enhance miR-146b levels, resulting in the attenuation of NF-κB activity and consequent amelioration of sepsis-induced kidney injury in mice[41] (Zhang et al). Nevertheless, the impact of BMSCs-Exo on SAKI remains unexplored.

Previous investigations have provided evidence the effectiveness of AMSCs-Exo (100 μg, 3 h post CLP) in ameliorating cerebral injury in septic rats.[42] Similarly, Gao et al[40] elucidated the protective attributes of AMSCs-Exo (100 μg, 4 h post CLP) against renal injury in septic mice. Our study demonstrates that treatment with BMSCs-Exo (100 μg, 3 h post CLP) effectively ameliorates renal pathology, enhances renal function, and improves survival rates among SAKI rats. Furthermore, the treatment with BMSCs-Exo led to a pronounced reduction in both inflammation and apoptosis levels in septic rats, mirroring

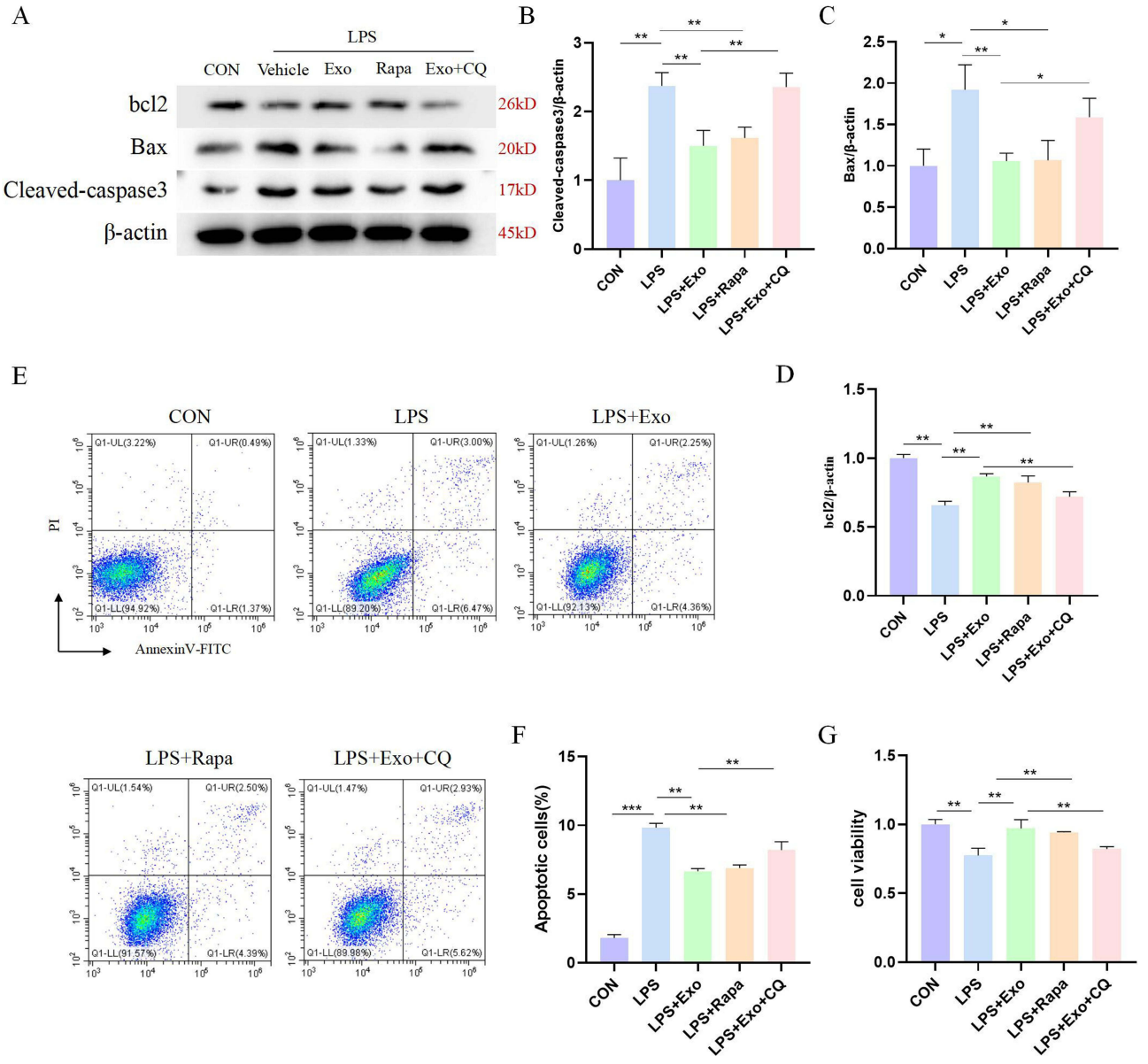

Figure 7 Evaluation of the role of Rapa and CQ on the anti-apoptotic effect of BMSCs-Exo. (**A**) Protein expression results of Cleaved-caspase 3, Bax, and bcl2 in five groups were determined by Western blot. (**B**–**D**) Relative quantitative analysis of protein levels in (**A**). (**E**) The flow cytometry showed the apoptotic rate of each group. (**F**) Statistical results of apoptotic rate. (**G**) HK-2 cell viability was detected by CCK-8 assay. *P< 0.05, **P< 0.01 and ***P< 0.001.

consistent outcomes observed in vitro. Importantly, we observed the internalization of BMSCs-Exo by renal cells, leading to their anti-inflammatory and anti-apoptotic contributions in the context of SAKI.

Numerous studies have underscored the involvement of autophagy in the pathogenesis of acute kidney injury, coupled with its intricate interplay with inflammation.[27,43,44] Within the autophagic process, LC3-I undergoes hydrolysis and conversion into LC3-II, culminating in the formation of autophagosomes.[45] This dynamic cellular catabolic process involves LC3-II conversion from LC3-I and the degradation of p62 through lysosomal fusion, thus the LC3-II/LC3-I ratio and p62 expression stand as reflective indicators of autophagic activity.[46] Notably, BMSCs-Exo have been shown to mitigate diabetic nephropathy (DN) by inducing autophagy in a rat model,[47] while pre-incubation with hucMSCs-Exo has been found to mitigate cisplatin-induced nephrotoxicity via autophagy activation.[48] In our current investigation, we observed upregulation of LC3-II/LC3-I and p62 expression both in LPS-treated HK-2 cells and kidney tissues from CLP-treated rats, indicative of heightened autophagosome formation, yet insufficient autolysosomal degradation. This phenomenon signifies an impediment in autophagic flux within

SAKI. Importantly, BMSCs-Exo intervention led to the upregulation of LC3-II/LC3-I and p62 expression, indicative of a mitigation in the obstructed autophagic flux. Nevertheless, inhibition of autophagy via CQ partially nullified the anti-inflammatory and anti-apoptotic effects of BMSCs-Exo in LPS-treated HK-2 cells. Furthermore, the effects of the autophagy activator Rapa were akin to those of BMSCs-Exo, encompassing the reduction of apoptosis and inflammation levels.

AMP-activated protein kinase (AMPK), a pivotal metabolic sensor, directly phosphorylates TSC2, an upstream regulator of the mammalian target of rapamycin (mTOR), thereby activating autophagy.[22] Extensive studies have highlighted the distinct roles of AMPK and mTOR in kidney physiology and disease.[49] Notably, the SAKI model has been associated with an increased p-AMPK/AMPK ratio and a decreased p-mTOR/mTOR ratio.[26,50] Our findings reveal that BMSCs-Exo further elevate the p-AMPK/AMPK ratio and reduce the p-mTOR/mTOR ratio, indicating the relief of obstructed autophagic flux through the AMPK/mTOR pathway. Previous research has demonstrated that sirtuin3 (SIRT3) safeguards against SAKI by inducing autophagy via AMPK/mTOR pathway regulation.[50] Additionally, AMPK/mTOR-mediated autophagy is implicated in the protective effects of Zinc-finger E-box-binding homeobox 1 (ZEB1) against SAKI. Moreover, a plethora of studies have substantiated AMPK activation's involvement in ischemia/reperfusion (I/R)-induced kidney injury[51–53] and cisplatin-induced nephrotoxicity.[54–56] Our study demonstrates that BMSCs-Exo alleviate inflammatory responses and apoptosis in the SAKI model, concomitant with alterations in autophagy-related and autophagic pathway-related proteins, suggesting that BMSCs-Exo alleviate SAKI by modulating autophagy via the AMPK/mTOR pathway.

Conclusion

This study unveils the potential protective role of BMSCs-Exo against SAKI, mediated by autophagy induction through the AMPK/mTOR pathway. These findings offer novel insights that could enhance the optimization of cell-free therapy for SAKI patients. However, our research has yet to elucidate the specific bioactive molecules of BMSCs-Exo that contribute to the renoprotective effects. Moreover, there are still numerous challenges in clinical applications of BMSCs-Exo. The details are as follows: 1. large-scale production of BMSCs-Exo; 2. evaluation of the safety and efficacy of BMSCs-Exo in clinical application; 3. engineered BMSCs-Exo to maximize cellular uptake and the biological information they deliver.

Acknowledgments

We thank the support received from Shanghai Jiao Tong University. This work was financially supported by the National Natural Science Foundation of China (No.82272245), the science and technology innovation project in Shanghai (No. SHDC22021203), and the medical innovation research project in Shanghai (No.21Y11902800).

Disclosure

The authors declare that they have no competing interests.

References

1. Yang L, Wang B, Ma L, Fu P. An update of long-noncoding RNAs in acute kidney injury. *Front Physiol*. 2022;13:849403. doi:10.3389/fphys.2022.849403
2. Hoste EAJ, Kellum JA, Selby NM, et al. Global epidemiology and outcomes of acute kidney injury. *Nat Rev Nephrol*. 2018;14(10):607–625. doi:10.1038/s41581-018-0052-0
3. Lu QB, Du Q, Wang HP, Tang ZH, Wang YB, Sun HJ. Salusin-β mediates tubular cell apoptosis in acute kidney injury: involvement of the PKC/ROS signaling pathway. *Redox Biol*. 2020;30:101411. doi:10.1016/j.redox.2019.101411
4. van der Poll T, van de Veerdonk FL, Scicluna BP, Netea MG. The immunopathology of sepsis and potential therapeutic targets. *Nat Rev Immunol*. 2017;17(7):407–420. doi:10.1038/nri.2017.36
5. Hümmeke-Oppers F, Hemelaar P, Pickkers P. Innovative drugs to target renal inflammation in sepsis: alkaline phosphatase. *Front Pharmacol*. 2019;10:919. doi:10.3389/fphar.2019.00919
6. Karbian N, Abutbul A, El-Amore R, et al. Apoptotic cell therapy for cytokine storm associated with acute severe sepsis. *Cell Death Dis*. 2020;11(7):535. doi:10.1038/s41419-020-02748-8
7. Zhu H, Wang X, Wang X, Liu B, Yuan Y, Zuo X. Curcumin attenuates inflammation and cell apoptosis through regulating NF-κB and JAK2/STAT3 signaling pathway against acute kidney injury. *Cell Cycle*. 2020;19(15):1941–1951. doi:10.1080/15384101.2020.1784599
8. Zhang B, Zeng M, Li B, et al. Arbutin attenuates LPS-induced acute kidney injury by inhibiting inflammation and apoptosis via the PI3K/Akt/Nrf2 pathway. *Phytomedicine*. 2021;82:153466. doi:10.1016/j.phymed.2021.153466
9. Jeppesen DK, Fenix AM, Franklin JL, et al. Reassessment of exosome composition. *Cell*. 2019;177(2):428–445.e418.

10. Ding C, Yi X, Wu X, et al. Exosome-mediated transfer of circRNA circnfix enhances temozolomide resistance in glioma. *Cancer Lett*. 2020;479:1–12. doi:10.1016/j.canlet.2020.03.002
11. Pitt JM, Charrier M, Viaud S, et al. Dendritic cell-derived exosomes as immunotherapies in the fight against cancer. *J Immunol*. 2014;193(3):1006–1011. doi:10.4049/jimmunol.1400703
12. Gao L, Wang L, Dai T, et al. Tumor-derived exosomes antagonize innate antiviral immunity. *Nat Immunol*. 2018;19(3):233–245. doi:10.1038/s41590-017-0043-5
13. Li H, Lu R, Pang Y, et al. Zhen-Wu-Tang protects iga nephropathy in rats by regulating exosomes to inhibit nf-κb/nlrp3 pathway. *Front Pharmacol*. 2020;11:1080. doi:10.3389/fphar.2020.01080
14. Bai L, Li J, Li H, et al. Renoprotective effects of artemisinin and hydroxychloroquine combination therapy on IgA nephropathy via suppressing NF-κB signaling and NLRP3 inflammasome activation by exosomes in rats. *Biochem Pharmacol*. 2019;169:113619. doi:10.1016/j.bcp.2019.08.021
15. Chen T, Wang C, Yu H, et al. Increased urinary exosomal microRNAs in children with idiopathic nephrotic syndrome. *EBioMedicine*. 2019;39:552–561. doi:10.1016/j.ebiom.2018.11.018
16. Lv LL, Feng Y, Wu M, et al. Exosomal miRNA-19b-3p of tubular epithelial cells promotes M1 macrophage activation in kidney injury. *Cell Death Differ*. 2020;27(1):210–226. doi:10.1038/s41418-019-0349-y
17. Li X, Liao J, Su X, et al. Human urine-derived stem cells protect against renal ischemia/reperfusion injury in a rat model via exosomal miR-146a-5p which targets IRAK1. *Theranostics*. 2020;10(21):9561–9578. doi:10.7150/thno.42153
18. Lange T, Artelt N, Kindt F, et al. MiR-21 is up-regulated in urinary exosomes of chronic kidney disease patients and after glomerular injury. *J Cell Mol Med*. 2019;23(7):4839–4843. doi:10.1111/jcmm.14317
19. Jiang T, Wang Z, Sun J. Human bone marrow mesenchymal stem cell-derived exosomes stimulate cutaneous wound healing mediates through TGF-β/Smad signaling pathway. *Stem Cell Res Ther*. 2020;11(1):198. doi:10.1186/s13287-020-01723-6
20. Liu L, Guo S, Shi W, et al. Bone marrow mesenchymal stem cell-derived small extracellular vesicles promote periodontal regeneration. *Tissue Eng Part A*. 2021;27(13–14):962–976. doi:10.1089/ten.tea.2020.0141
21. Zhu G, Pei L, Lin F, et al. Exosomes from human-bone-marrow-derived mesenchymal stem cells protect against renal ischemia/reperfusion injury via transferring miR-199a-3p. *J Cell Physiol*. 2019;234(12):23736–23749. doi:10.1002/jcp.28941
22. Gong L, Pan Q, Yang N. Autophagy and inflammation regulation in acute kidney injury. *Front Physiol*. 2020;11:576463. doi:10.3389/fphys.2020.576463
23. Zhao XC, Livingston MJ, Liang XL, Dong Z. Cell apoptosis and autophagy in renal fibrosis. *Adv Exp Med Biol*. 2019;1165:557–584.
24. Ye X, Chen L. Protective role of autophagy in triptolide-induced apoptosis of TM3 leydig cells. *J Transl Med*. 2023;11(3):265–274. doi:10.2478/jtim-2021-0051
25. Zhao J, Zheng H, Sui Z, et al. Ursolic acid exhibits anti-inflammatory effects through blocking TLR4-myd88 pathway mediated by autophagy. *Cytokine*. 2019;123:154726. doi:10.1016/j.cyto.2019.05.013
26. Tan C, Gu J, Li T, et al. Inhibition of aerobic glycolysis alleviates sepsis-induced acute kidney injury by promoting lactate/sirtuin 3/AMPK-regulated autophagy. *IntJ Mol Med*. 2021;47(3):doi:10.3892/ijmm.2021.4852
27. Cui J, Bai X, Chen X. Autophagy and acute kidney injury. *Adv Exp Med Biol*. 2020;1207:469–480.
28. Zuo Z, Li Q, Zhou S, et al. Berberine ameliorates contrast-induced acute kidney injury by regulating HDAC4-FoxO3a axis-induced autophagy: in vivo and in vitro. *Phytother Res*. 2023. doi:10.1002/ptr.8059
29. Dikic I, Elazar Z. Mechanism and medical implications of mammalian autophagy. *Nat Rev Mol Cell Biol*. 2018;19(6):349–364. doi:10.1038/s41580-018-0003-4
30. Inoki K, Zhu T, Guan KL. TSC2 mediates cellular energy response to control cell growth and survival. *Cell*. 2003;115(5):577–590. doi:10.1016/S0092-8674(03)00929-2
31. González A, Hall MN. Nutrient sensing and TOR signaling in yeast and mammals. *EMBO J*. 2017;36(4):397–408. doi:10.15252/embj.201696010
32. Hua T, Yang M, Song H, et al. Huc-MSCs-derived exosomes attenuate inflammatory pain by regulating microglia pyroptosis and autophagy via the miR-146a-5p/TRAF6 axis. *J Nanobiotechnol*. 2022;20(1):324. doi:10.1186/s12951-022-01522-6
33. Ji Y, Xiong L, Zhang G, et al. Synovial fluid exosome-derived miR-182-5p alleviates osteoarthritis by downregulating TNFAIP8 and promoting autophagy through LC3 signaling. *Int Immunopharmacol*. 2023;125(Pt A):111177. doi:10.1016/j.intimp.2023.
34. Jin C, Cao YM, Shang JW, Li YC. Protective effects of exosomes derived from bone mesenchymal stem cells in sepsis-induced acute kidney injury cell model in vitro. *J Tongji Univ*. 2022;43(02):157–164. in Chinese.
35. Friedenstein AJ, Chailakhyan RK, Gerasimov UV. Bone marrow osteogenic stem cells: in vitro cultivation and transplantation in diffusion chambers. *Cell Tissue Kinet*. 1987;20(3):263–272. doi:10.1111/j.1365-2184.1987.tb01309.x
36. Pegtel DM, Gould SJ. Exosomes. *Annu Rev Biochem*. 2019;88(1):487–514. doi:10.1146/annurev-biochem-013118-111902
37. Mashouri L, Yousefi H, Aref AR, Ahadi AM, Molaei F, Alahari SK. Exosomes: composition, biogenesis, and mechanisms in cancer metastasis and drug resistance. *Mol Cancer*. 2019;18(1):75. doi:10.1186/s12943-019-0991-5
38. Raeven P, Zipperle J, Drechsler S. Extracellular vesicles as markers and mediators in sepsis. *Theranostics*. 2018;8(12):3348–3365. doi:10.7150/thno.23453
39. Jin X, Sun H, Yang L. How extracellular nano-vesicles can play a role in sepsis? An evidence-based review of the literature. *Int j Nanomed*. 2023;18:5797–5814. doi:10.2147/IJN.S427116
40. Gao F, Zuo B, Wang Y, Li S, Yang J, Sun D. Protective function of exosomes from adipose tissue-derived mesenchymal stem cells in acute kidney injury through SIRT1 pathway. *Life Sci*. 2020;255:117719. doi:10.1016/j.lfs.2020.117719
41. Zhang R, Zhu Y, Li Y, et al. Human umbilical cord mesenchymal stem cell exosomes alleviate sepsis-associated acute kidney injury via regulating microRNA-146b expression. *Biotechnol Lett*. 2020;42(4):669–679. doi:10.1007/s10529-020-02831-2
42. Chang CL, Chen HH, Chen KH, et al. Adipose-derived mesenchymal stem cell-derived exosomes markedly protected the brain against sepsis syndrome induced injury in rat. *Am J Transl Res*. 2019;11(7):3955–3971.
43. Kaushal GP, Shah SV. Autophagy in acute kidney injury. *Kidney Int*. 2016;89(4):779–791.
44. Kimura T, Isaka Y, Yoshimori T. Autophagy and kidney inflammation. *Autophagy*. 2017;13(6):997–1003. doi:10.1080/15548627.2017.1309485
45. Chen Y, Song F. Research advances in selective adaptor protein autophagy of p62/sequestosome-1. *Chin J Pharmacol Toxicol*. 2016;30(3):258–265.

46. Yue Z, Guan X, Chao R, et al. Diallyl disulfide induces apoptosis and autophagy in human osteosarcoma mg-63 cells through the pi3k/akt/mtor pathway. *Molecules*. 2019;24(14):doi:10.3390/molecules24142665
47. Ebrahim N, Ahmed IA, Hussien NI, et al. Mesenchymal stem cell-derived exosomes ameliorated diabetic nephropathy by autophagy induction through the mtor signaling pathway. *Cells*. 2018;7(12):226. doi:10.3390/cells7120226
48. Wang B, Jia H, Zhang B, et al. Pre-incubation with hucMSC-exosomes prevents cisplatin-induced nephrotoxicity by activating autophagy. *Stem Cell Res Ther*. 2017;8(1):75. doi:10.1186/s13287-016-0463-4
49. Rajani R, Pastor-Soler NM, Hallows KR. Role of AMP-activated protein kinase in kidney tubular transport, metabolism, and disease. *Curr Opin Nephrol Hypertens*. 2017;26(5):375–383. doi:10.1097/MNH.0000000000000349
50. Zhao W, Zhang L, Chen R, et al. SIRT3 protects against acute kidney injury via AMPK/mTOR-regulated autophagy. *Front Physiol*. 2018;9:1526. doi:10.3389/fphys.2018.01526
51. Gwon DH, Hwang TW, Ro JY, et al. High endogenous accumulation of ω-3 polyunsaturated fatty acids protect against ischemia-reperfusion renal injury through AMPK-mediated autophagy in fat-1 mice. *Int J Mol Sci*. 2017;18(10):2081. doi:10.3390/ijms18102081
52. Chen BL, Wang LT, Huang KH, Wang CC, Chiang CK, Liu SH. Quercetin attenuates renal ischemia/reperfusion injury via an activation of AMP-activated protein kinase-regulated autophagy pathway. *J Nutr Biochem*. 2014;25(11):1226–1234. doi:10.1016/j.jnutbio.2014.05.013
53. Wang LT, Chen BL, Wu CT, Huang KH, Chiang CK, Hwa Liu S. Protective role of AMP-activated protein kinase-evoked autophagy on an in vitro model of ischemia/reperfusion-induced renal tubular cell injury. *PLoS One*. 2013;8(11):e79814. doi:10.1371/journal.pone.0079814
54. Park YJ, Kim KS, Park JH, et al. Protective effects of dendropanoxide isolated from dendropanax morbifera against cisplatin-induced acute kidney injury via the AMPK/mTOR signaling pathway. *Food Chem Toxicol*. 2020;145:111605. doi:10.1016/j.fct.2020.111605
55. Xing JJ, Hou JG, Ma ZN, et al. Ginsenoside Rb3 provides protective effects against cisplatin-induced nephrotoxicity via regulation of AMPK-/mTOR-mediated autophagy and inhibition of apoptosis in vitro and in vivo. *Cell Proliferation*. 2019;52(4):e12627. doi:10.1111/cpr.12627
56. Kim TW, Kim YJ, Kim HT, et al. NQO1 deficiency leads enhanced autophagy in cisplatin-induced acute kidney injury through the AMPK/TSC2/mTOR signaling pathway. *Antioxid. Redox Signaling*. 2016;24(15):867–883. doi:10.1089/ars.2015.6386